

Electrically-Driven Catalytic Alkane Dehydrogenation As A Means For
Renewable Hydrogen Fuel

Ariana B. Nygren

Department of Chemistry

University of Colorado, Boulder

Defense Date: 18 March 2024

Thesis Advisor: Dr. Oana Luca

Defense Committee:

Dr. Oana Luca, Department of Chemistry, University of Colorado Boulder

Dr. Veronica Vaida, Department of Chemistry, University of Colorado Boulder

Dr. Harrison Carpenter, Department of Ecology and Evolutionary Biology, University of
Colorado Boulder

Table of Contents

Acknowledgements	2
Abstract	3
Introduction	4
Experimental Methods	
Synthesis of the Iridium CCC-Pincer Complex	8
¹ H-NMR For Complex Identification and Classification	12
Gas Chromatography	12
In Situ Octane Dehydrogenation	13
Results and Discussion	
Synthesis of the Iridium CCC-Pincer Complex	14
Quantification of the Octane Dehydrogenation	20
Conclusion	21
References	22
Appendix	24

Acknowledgements

Firstly, I would like to express my gratitude to my Primary Investigator and supervisor, Dr. Oana Luca, for her continuous advice and mentoring throughout the entirety of my research. Her input and leadership allowed me to both expand my knowledge and improve my work as a researcher as a whole. In addition, I would like to offer a special thanks to my graduate student mentor, Hunter Koltunski, for his guidance with the project as a whole as well as his teachings in chemistry concepts and research that I lacked in prior. I was able to gain far more experience and knowledge as a result of his help. I would also like to thank the other graduate students of the Luca lab, Phil (Phuc) Pham and Haley Petersen, for their additional help in the lab. Overall, I express my sincere thanks to all of the researchers in the Luca lab who have helped me along the way.

Abstract

The increasing threat of the burning of fossil fuels and its contribution to global warming has led to the increasing focus on a new means for the utilization and storage of clean and renewable energy^{1,2}. Hydrogen fuel cells are at the forefront of research in this field³. In the chemistries of such fuel cells, the only products of these devices are energy is water⁴. However, with the use of hydrogen gas, several safety drawbacks are found: high flammability, invisible flame, and ability to embrittle metal⁵, therefore an improved way of storage that does not involve the gas itself has been sought after. One proposed solution has been to store the hydrogen in chemical bonds^{6,7}. Previous research has shown an effective method being through a catalytic dehydrogenation reaction of alkanes to produce hydrogen^{6,7}. This reaction has been performed at high temperatures^{7,8}, which is inapplicable on a larger scale. The aim of my research is to perform acceptorless dehydrogenation of alkanes at ambient temperatures to produce and release hydrogen from alkane chemical bonds. An iridium pincer catalyst with a sigma-donating cyclic N-heterocyclic carbene containing ligand, called the CCC ligand, was used to perform the reaction⁸. To do so, a reducing agent in dimeric form, [N-DMBI]₂, was used to reduce the iridium pincer catalyst so it can be activate for the dehydrogenation reaction. Through proving this concept, the same reaction can then be done using electrochemical methods. Two reactions were set up containing the iridium CCC-pincer complex and octane, one with the N-DMBI and one without. The content of octane and 1-octene in each reaction was analyzed and quantified using flame ionization detector gas chromatography (GC-FID). In doing so, both reaction mixtures showed the presence of 1-octene. However, the reaction mixture containing N-DMBI had a greater amount of 1-octene than without, indicating the reduction of the iridium metal center by the N-DMBI.

Introduction

The most widely used form of energy for both power plants and commercial vehicles, specifically combustion engines, is the burning of fossil fuels. It has been a readily available resource in the form of coal, oil, and natural gas^{1,2}. However, this reaction releases harmful carbon dioxide, a greenhouse gas, into the atmosphere^{1,2}. The greater implication of this is the further increase of global warming, adding further danger to the sanctity of the environment^{1,2}. The increasing threat of fossil fuels and their impact on the environment has resulted in a desperate need for an alternative, clean form of energy and energy storage. A means of energy without the release of greenhouse gasses into the atmosphere has been highly sought after. At the forefront of clean and renewable energy research has been hydrogen fuel cells from water electrolysis^{3,4}. The only byproduct of this reaction aside from heat is water, making it one of the most clean forms of green energy^{3,4}.

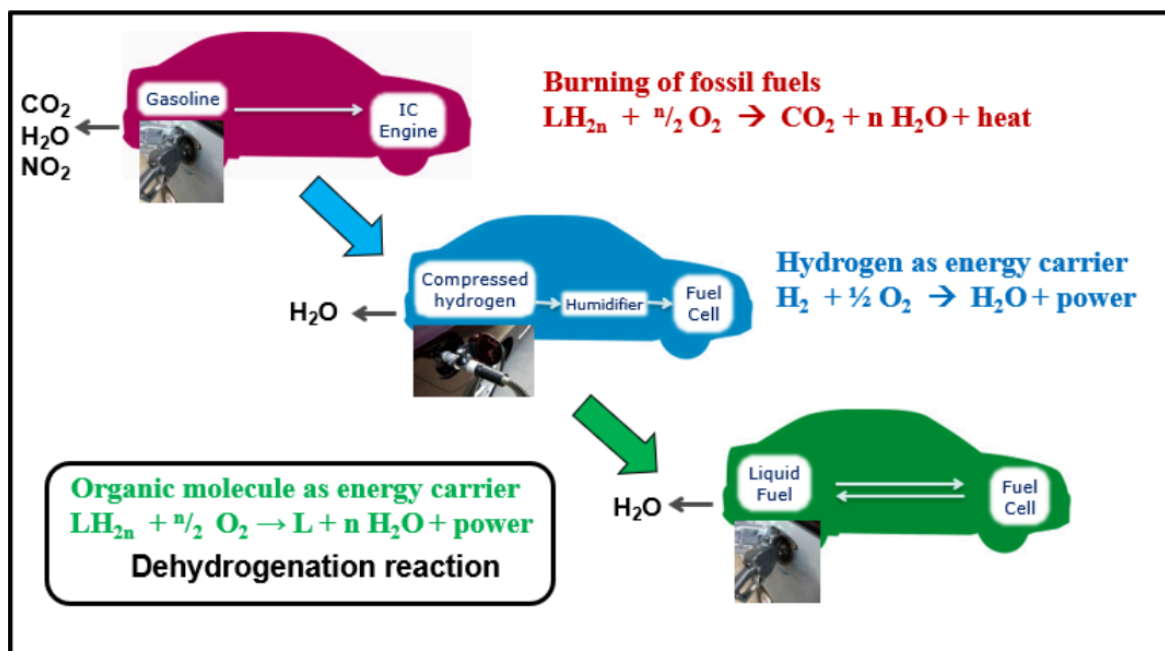


Figure 1: A diagram showing the reactants and products resulting from different forms of energy and energy carriers.

Despite its many sought after qualities, hydrogen fuel still has its setbacks. The most prominent issue involving this reaction is the danger of hydrogen gas. Hydrogen gas is highly flammable, shows a nearly invisible flame, and embrittles the metal containers that it's stored in⁵. Storing such a gas would be far too dangerous, given the potential of ignition, explosions, and leaks⁵. A way to address this issue is to store the hydrogen in chemical bonds that can be released when needed^{6,7}.

Research thus far has indicated liquid organic hydrogen carriers (LOHC's) as a promising form of H₂ storage^{6,7}. They result in a reversible dehydrogenation/hydrogenation reaction of the C-C bonds in liquid hydrocarbons^{6,7}. Literature has shown that organometallic pincer complexes can perform the dehydrogenation reaction on alkanes to produce alkenes and H₂⁸. This reaction is energy intensive and difficult to perform at ambient temperatures and pressure⁶⁻⁸. The use of the high temperatures and pressures needed for the reaction would be inefficient on a large scale, resulting in a large setback of hydrogen fuel. In addition, the reaction has been done using "acceptor" molecules, as a means for transfer hydrogen⁹. Since the hydrogen is transferred from one molecule to another, it limits the generation of hydrogen.

Previous research has proven iridium complexes with sigma-donating cyclic N-heterocyclic carbene containing ligands to be capable of performing "acceptorless" dehydrogenation of alkanes under high temperatures and using caustic catalyst activators^{8,10,11}. Iridium is very reactive in oxidative addition, making it effective in the sought after dehydrogenation reaction^{8,10,11}.

To remedy the current setbacks of hydrogen fuel cells, my research proposes to demonstrate reversible electricity-driven hydrogen storage within the structure of organic molecules. This will be done using the general catalytic cycle shown in Figure 2.

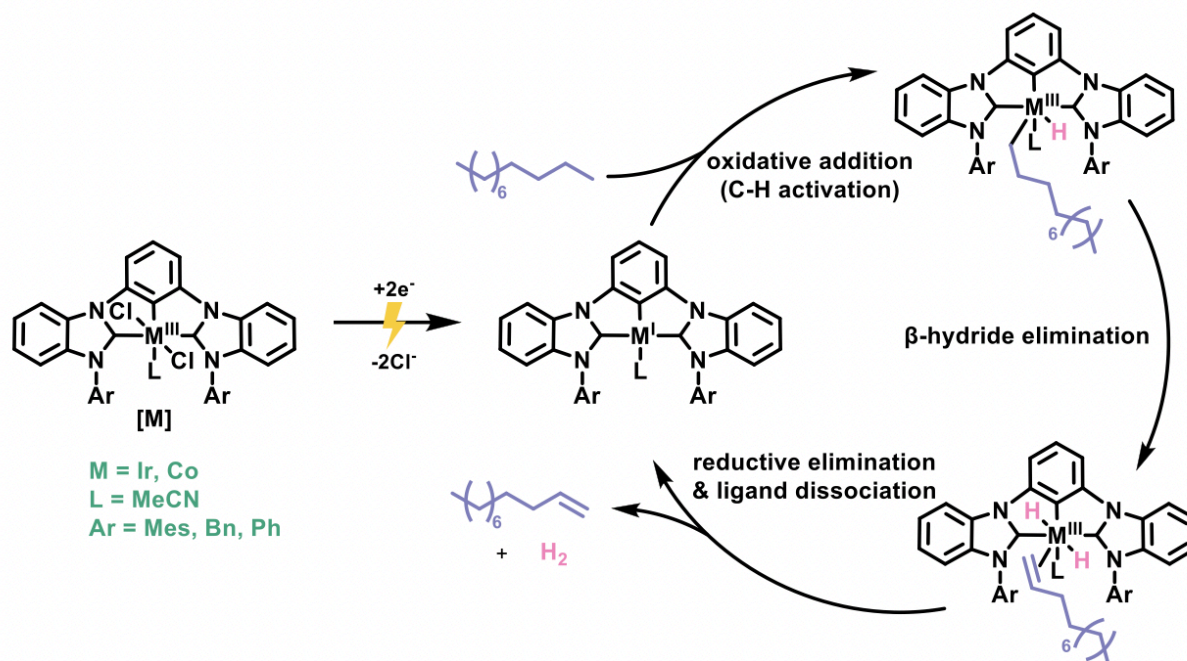


Figure 2: The general dehydrogenation catalytic cycle of an alkane to produce H_2 .

My research aims to prove that, by the addition of a reducing agent to the reaction reported in previous literature, the redox reaction outlined in Figure 2 is possible and will produce H_2 .

The chosen reducing agent is 4-(1,3-Dimethyl-2,3-dihydro-1H-benzoimidazol-2-yl)phenyl)dimethylamine, otherwise known as N-DMBI^{12,13}. This was chosen because it was readily available, stable with oxidation, and doesn't require an inert atmosphere, making redox reactions easier^{12,13}. In addition, only one equivalent will need to be used to reduce the iridium, since it's a dimer that can donate two electrons¹². Therefore, my hypothesis is that the N-DMBI will reduce the Ir^{III} to Ir^{I} so that the redox reaction in Figure 2 is able to occur. The revised mechanism is shown in Figure 3.

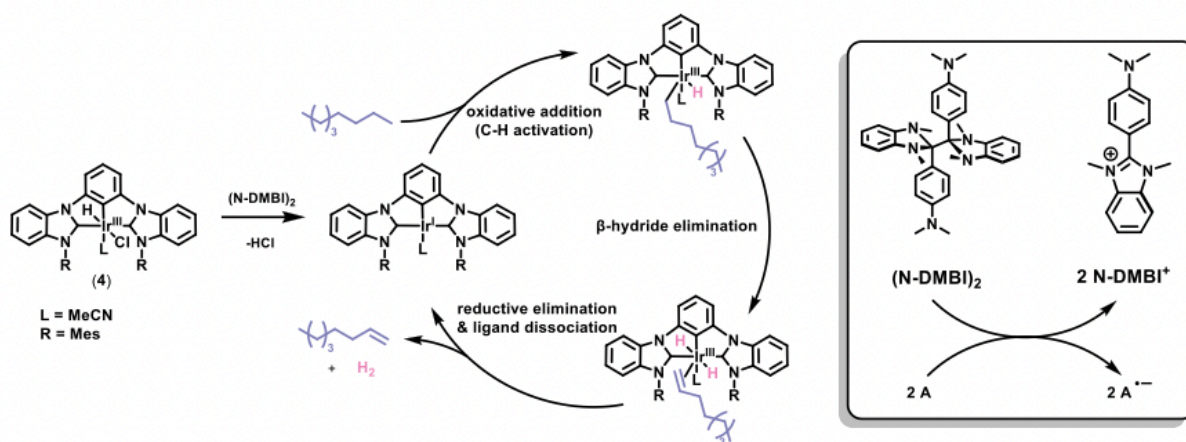


Figure 3: The general dehydrogenation catalytic cycle of an alkane to produce H₂, inclusive of the reduction of the iridium, labeled as “A”.

This redox reaction is done in an “acceptorless” fashion, where the H₂ is released rather than transferred, allowing for H₂ to be stored and released when needed^{12,13}.

The overall hypothesis of my research is that if the N-DMBI is able to reduce the iridium, resulting in the proposed redox reaction at ambient temperature and pressure, the same reaction can be replicated using electrochemical methods.

Experimental Methods

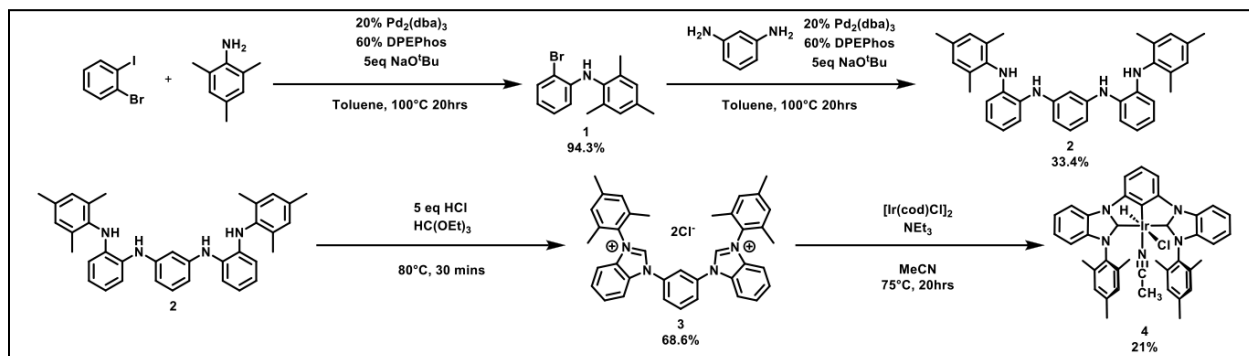
Synthesis of the Iridium CCC-Pincer Complex

Figure 4: The overall reaction scheme, as well as percent yield of each step of the synthesis.

To synthesize the CCC-pincer complex, first the ligand was synthesized. To do so, the schlenk line method was used. The synthesis was broken into parts. The first was a cross coupling reaction connecting 2-bromoiodobenzene and 2,4,6-trimethylaniline to form N-(2-bromophenyl)-2,4,6-trimethylaniline (**1**).

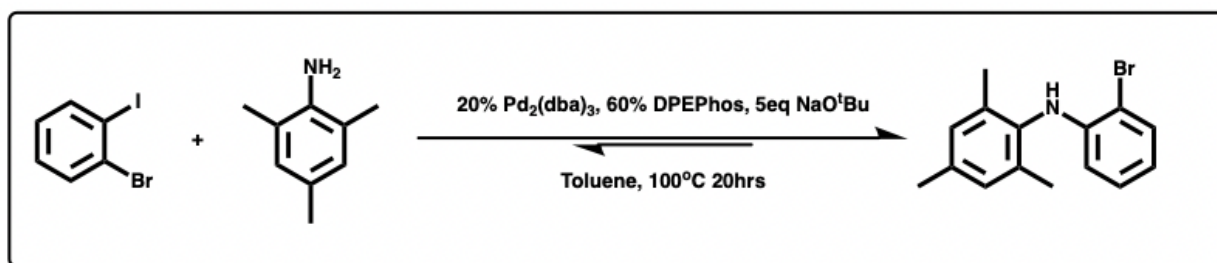


Figure 5: The cross-coupling reaction to form N-(2-bromophenyl)-2,4,6-trimethylaniline, using a palladium catalyst.

This compound was prepared by a modification of a published method¹⁴; its identity was verified by comparing the ¹H NMR spectrum with literature data. Tris(dibenzylideneacetone) dipalladium (0.347 mmol, 317.87 mg) and DPEPhos (1.07 mmol, 576.68 mg) were added to a flame-dried Schlenk flask. Toluene (25 mL) was added under argon, and the solution was stirred at room temperature for 10 minutes, changing from a dark red to a red orange solution.

2-bromiodobenzene (10.5 mmol, 1.35 mL), and 2,4,6-trimethylaniline (7.12 mmol, 1.00 mL) were added via syringe. The flask was opened under a backflow of argon and sodium tert-butoxide (28.17 mmol, 2.7078 g) was added. The septum was replaced, and any residual solid not in the solution was washed down with 25 mL of toluene added via syringe. The mixture was stirred for 20 hours at 100 °C, and then allowed to cool to room temperature. The mixture was diluted with 50 mL diethyl ether and filtered through a plug of silica gel, eluting with ether. The solvent was evaporated, and the residue was purified by flash chromatography with 10% ethyl acetate in hexanes as eluent. The product yielded was a white solid. Yield: 1.94327 g, 94.3%. ¹H NMR (300 MHz, CDCl₃) δ 7.50 (dd, *J* = 7.9, 1.4 Hz, 1H), 7.10 – 6.98 (m, 1H), 7.00 (d, *J* = 8.8 Hz, 2H), 6.67 – 6.55 (m, 1H), 6.18 (dt, *J* = 8.2, 1.4 Hz, 1H), 5.64 (s, 1H), 2.35 (s, 3H), 2.19 (s, 6H).

The N-(2-bromophenyl)-2,4,6-trimethylaniline then went through a cross-coupling reaction with m-phenylenediamine to produce what we call the CCC backbone, named N¹,N^{1'}-(1,3-phenylene)bis(N²-mesitylbenzene-1,2-diamine). (2).

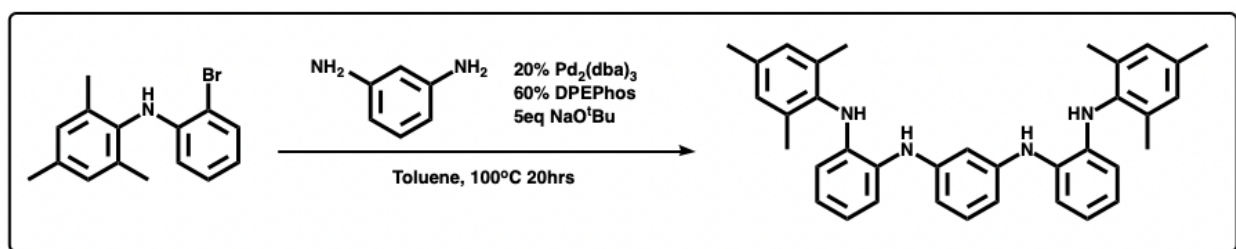


Figure 6: The cross-coupling reaction of N-(2-bromophenyl)-2,4,6-trimethylaniline and m-phenylenediamine to produce the CCC backbone.

This compound was prepared by a modification of a published method; its identity was verified by comparing the ¹H NMR spectrum with literature data¹⁴. Tris(dibenzylideneacetone) dipalladium (0.4 mmol, 366 mg) and DPEPhos (1.2 mmol, 645 mg) were added to a flame-dried

Schlenk flask. Toluene (25 mL) was added under argon, and the solution was stirred at room temperature for 10 minutes, changing from a dark red to a red orange solution. The flask was opened under a backflow of argon and Compound **(1)** (4.4 mmol, 1.276 g), 1,3-diaminobenzene (2.0 mmol, 216.38 mg), and sodium tert-butoxide (11.96 mmol, 1.15 g) were added. The septum was replaced, and any residual solid not in the solution was washed down with 25 mL of toluene added via syringe. The mixture was stirred for 20 hours at 100 °C, and then allowed to cool to room temperature. The mixture was diluted with 50 mL diethyl ether and filtered through a plug of silica gel, eluting with ether. The solvent was evaporated, and the residue was purified by flash chromatography with 10% ethyl acetate in hexanes as eluent. The product yielded was a yellow-green solid. Yield: 388.06 mg, 33.4%. $^1\text{H NMR}$ (300 MHz, CDCl_3) δ 7.47 (dd, $J = 7.9$, 1.6 Hz, 2H), 7.07 – 6.96 (m, 2H), 6.95 (s, 5H), 6.58 (td, $J = 7.6$, 1.6 Hz, 2H), 6.15 (dd, $J = 8.1$, 1.6 Hz, 2H), 5.63 (s, 2H), 2.31 (s, 6H), 2.16 (s, 10H).

The final step to the synthesis of the ligand is to form what we call the CCC pincer, named 1,1'-(1,3-phenylene)bis(3-mesityl-1H-benzo[d]imidazol-3-ium) chloride (**3**).

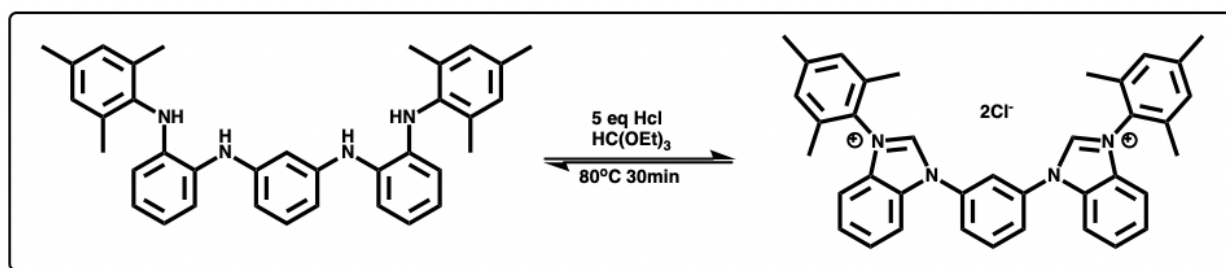


Figure 7: The reaction of the CCC backbone to form the CCC ligand.

This compound was prepared by a modification of a published method; its identity was verified by comparing the $^1\text{H NMR}$ spectrum with literature data¹⁴. Compound **(2)** (0.74 mmol, 388.06 mg) was dissolved in 15 mL triethyl orthoformate. Concentrated hydrochloric acid (37% w/w, 5.2 mmol, 0.16 mL of solution) was added, which resulted in the formation of a purple

solution. The mixture was stirred at 80 °C for 2 hours and an off-white precipitate was noted. The reaction mixture was cooled to room temperature and diluted with 20 mL ether, followed by 40 mL pentane. The solid was collected by filtration and washed with excess ether. Yield: 313.03 mg, 68.6%. ¹H NMR (300 MHz, CDCl₃) δ 12.05 (s, 2H), 8.97 (s, 1H), 8.53 (d, *J* = 8.1 Hz, 2H), 8.33 (d, *J* = 7.4 Hz, 2H), 8.21 (s, 1H), 7.84 (d, *J* = 7.6 Hz, 2H), 7.67 (t, *J* = 7.7 Hz, 2H), 7.32 (d, *J* = 8.3 Hz, 2H), 7.10 (s, 4H), 2.39 (s, 6H), 2.13 (s, 13H).

Finally, the iridium CCC-pincer complex (**4**) was synthesized.

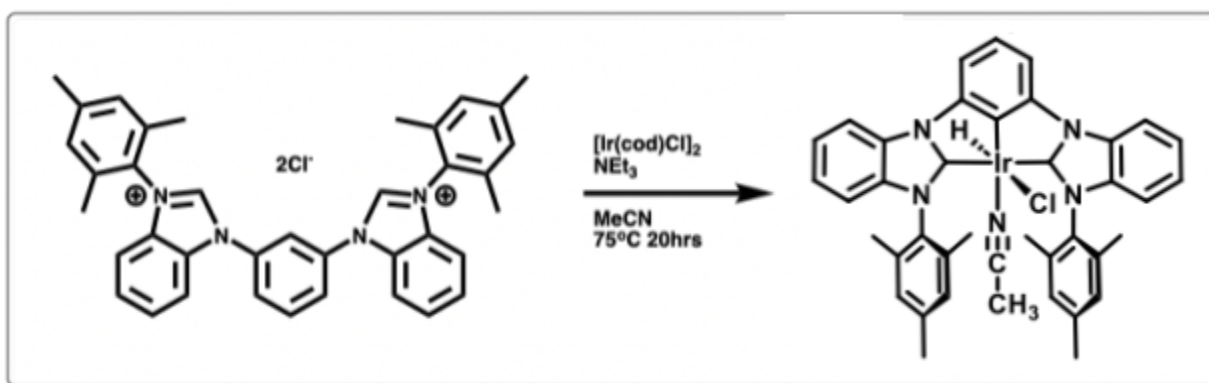


Figure 8: The metalation of the CCC pincer to form the iridium CCC-pincer complex.

This compound was prepared by a modification of a published method; its identity was verified by comparing the ¹H NMR spectrum with literature data¹⁴. Compound (**3**) (0.079 mmol, 49.22 mg) and [Ir(cod)Cl]₂ (0.040 mmol, 27.21 mg) were added to a flame-dried Schlenk flask fixed with a flame dried addition funnel. The setup was evacuated and backfilled with argon. Acetonitrile (12 mL) was added, and the reaction mixture was heated to 80 °C. A solution of triethylamine (7.17 mmol, 1 mL) in acetonitrile (12.5 mL) was added dropwise over an hour. The reaction was stirred at 80 °C for 10 h. The solvent was evaporated, and the residue was purified by column chromatography on activated alumina, using a gradient of 0 to 30 % ethyl acetate in dichloromethane. The product yielded was a neon-yellow solid. Yield: 6.8 mg, 21% ¹H NMR

(300 MHz, CD_2Cl_2) δ 8.17 (dt, $J = 8.2, 0.9$ Hz, 2H), 7.68 (d, $J = 7.9$ Hz, 2H), 7.44 (ddd, $J = 8.3, 7.4, 1.1$ Hz, 2H), 7.36 – 7.22 (m, 3H), 7.05 (d, $J = 1.7$ Hz, 2H), 7.03 – 6.98 (m, 2H), 6.95 (dt, $J = 7.9, 1.0$ Hz, 2H), 2.34 (s, 6H), 2.22 (s, 6H), 1.95 (s, 6H), 1.43 (s, 3H), -23.20 (s, 1H).

¹H-NMR For Complex Identification and Classification

¹H-NMR was used to identify and classify the compounds of each step of the synthesis as well as ensure their purity. Specifically, ¹H-NMR was used to identify the iridium CCC-pincer complex through its expected hydride peak.

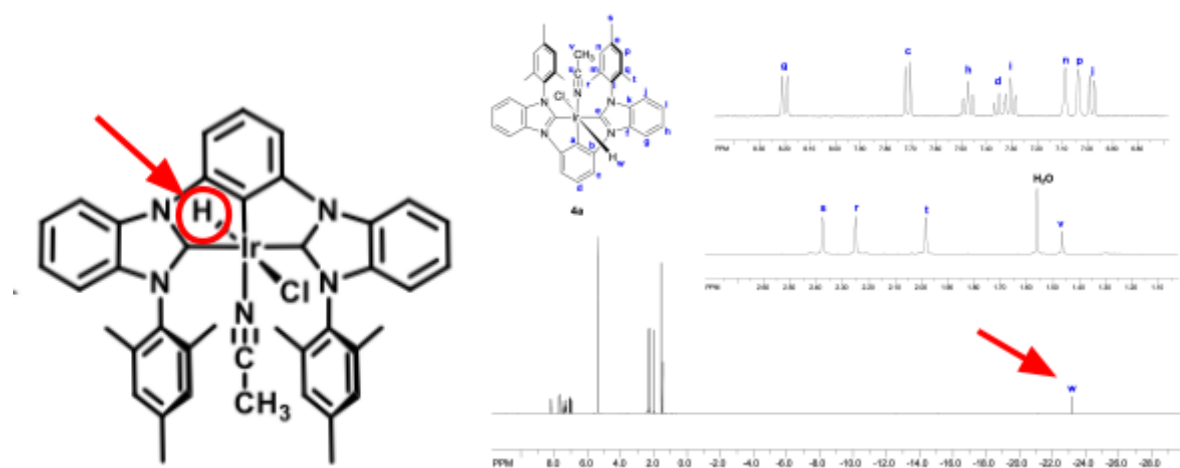
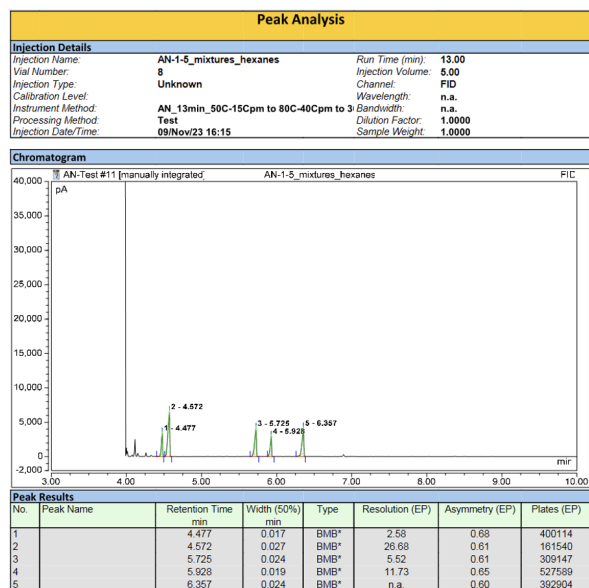


Figure 9: The expected hydride peak of the iridium CCC-pincer complex¹⁴.

Gas Chromatography

To quantify the amount of alkane and alkene in the dehydrogenation reaction, flame ionization detector gas chromatography (GC-FID) was used. Two alkanes were used to analyze the dehydrogenation reaction, those being octane and cyclooctane, with their respective alkenes. Four calibration curves of octane, 1-octene, cyclooctane, and cyclooctene, using mesitylene as the internal standard and cyclohexane as the solvent were made. Eight standards were made of

concentrations of 0.05 mM, 0.25 mM, 0.5 mM, 1.0 mM, 1.5 mM, 2.5 mM, 4.0 mM, and 5.0 mM. In addition, all of the alkanes, alkenes, and mesitylene at approximately 1 mM concentration were run to ensure good separation of the peaks.



Instrument method

Injection volume: 5 μ L

Temperature profile:

- 50 $^{\circ}$ C, hold 2 min
- Ramping 15 $^{\circ}$ C/min to 80 $^{\circ}$ C, hold 1 min
- Ramping 40 $^{\circ}$ C/min to 300 $^{\circ}$ C, hold 2.5 min
- Total analysis time: 13 min

Notes

Retention time: each compound is approximately 1 mM. Good separation for octane and octene

- Octene: 4.477
- Octane: 4.572
- Cyclooctene (*cis* isomer): 5.725
- Cyclooctane: 5.928
- Mesitylene (internal standard): 6.357

Figure 10: The instrumentation method and retention times of each compound in the mixture, including the internal standard.

The retention times in Figure 10 were used to differentiate the peaks present in the in situ octane dehydrogenation reaction.

In Situ Octane Dehydrogenation

The iridium CCC-pincer complex was synthesized as described above and shown in Figure 6 in two separate reaction flasks. To one of the flasks, 0.9 mL of octane was added as a standard, to show the reaction without the reducing agent. To the other, 0.9 mL of octane was added alongside one equivalent of (N-DMBI)₂. The solution was stirred at 80 $^{\circ}$ C and a color change from orange to bright yellow was observed. Mesitylene was added to both solutions and both solutions were analyzed using GC-FID, with the instrument method in Figure 10.

Results and Discussion

Synthesis of the Iridium CCC-Pincer Complex

To ensure the correct product was being produced, as well as the greatest yield possible was attained, $^1\text{H-NMR}$ was run for each step of the process. Each was run in deuterated chloroform. Firstly, the NMR of the N-(2-bromophenyl)-2,4,6-trimethylaniline:

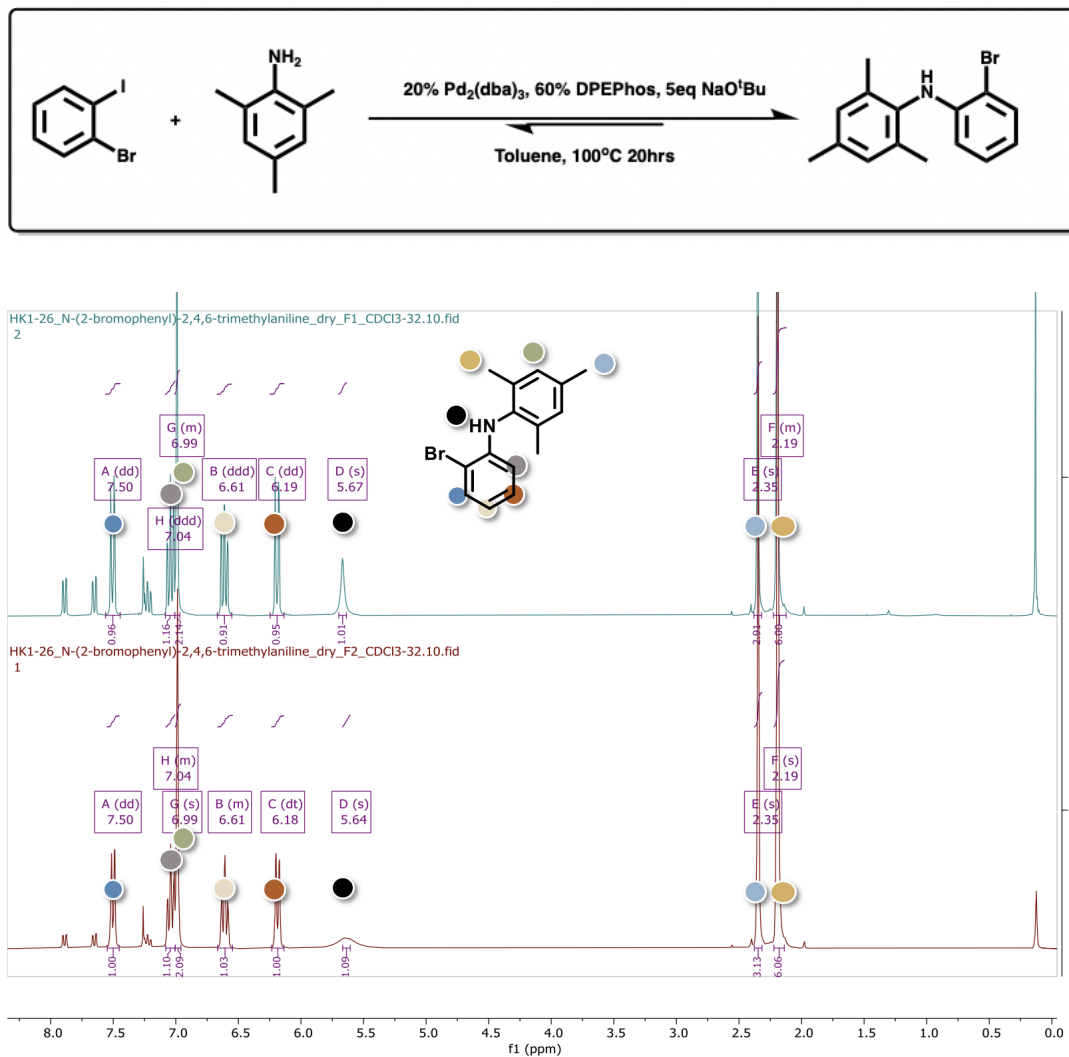


Figure 11: The NMR of Compound (**1**) with peak assignments.

The NMR of the two fractions were clean and showed the correct product. The spectra ranges from 2.0 ppm, where the methyl groups reside, to 8.0 ppm, where the cyclic groups

reside. The yield was 94.3%. So, we proceeded with the next step. This was the synthesis of compound (2).

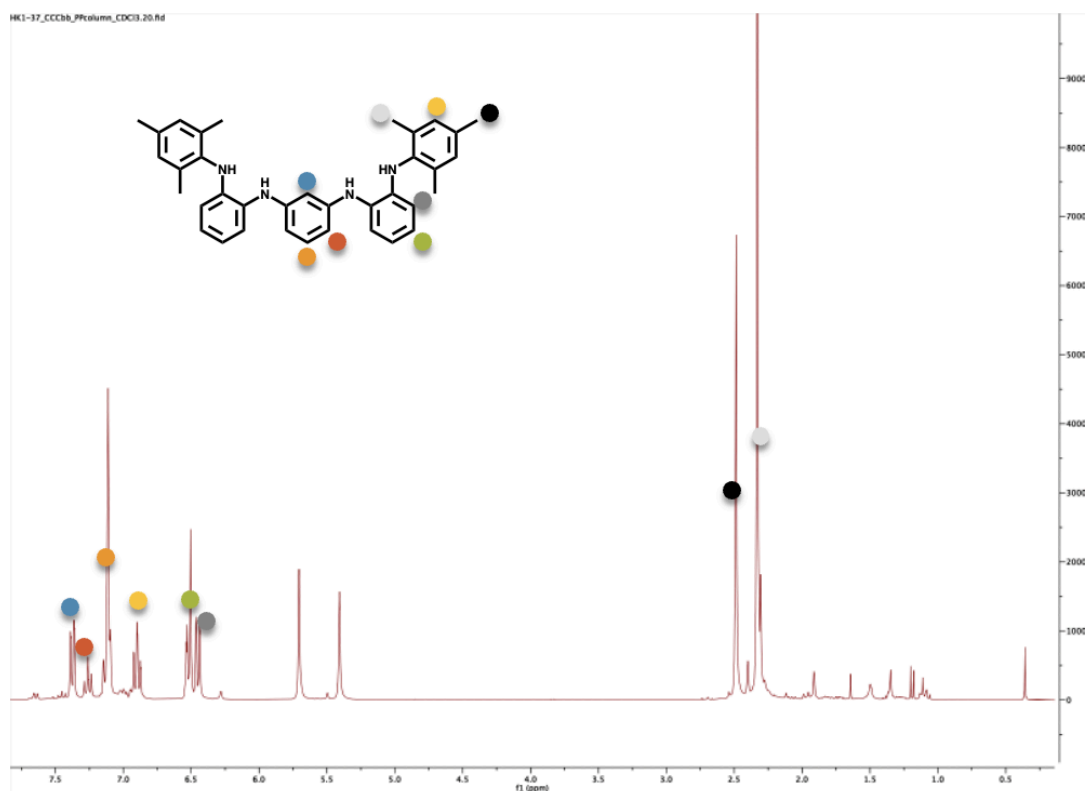
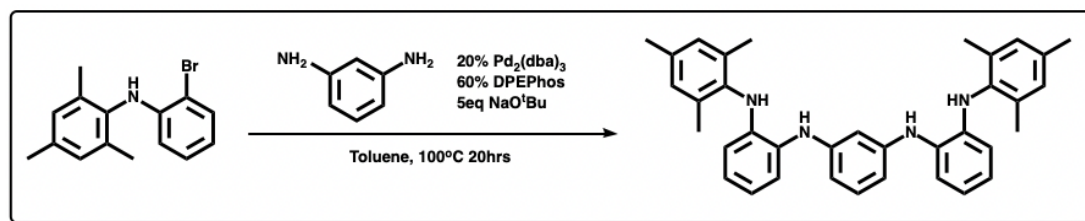


Figure 12: The NMR of Compound (2) with peak assignments.

The NMR showed the correct product. Similar to the step prior, the methyl groups sat around 2.5 ppm and the cyclic groups ranged from 6.5-7.5 ppm. However, as evident by the many extra peaks, there were still some impurities left in the product. In addition, the yield was 33.4%. Still, we proceeded with the next step, the synthesis of Compound (3).

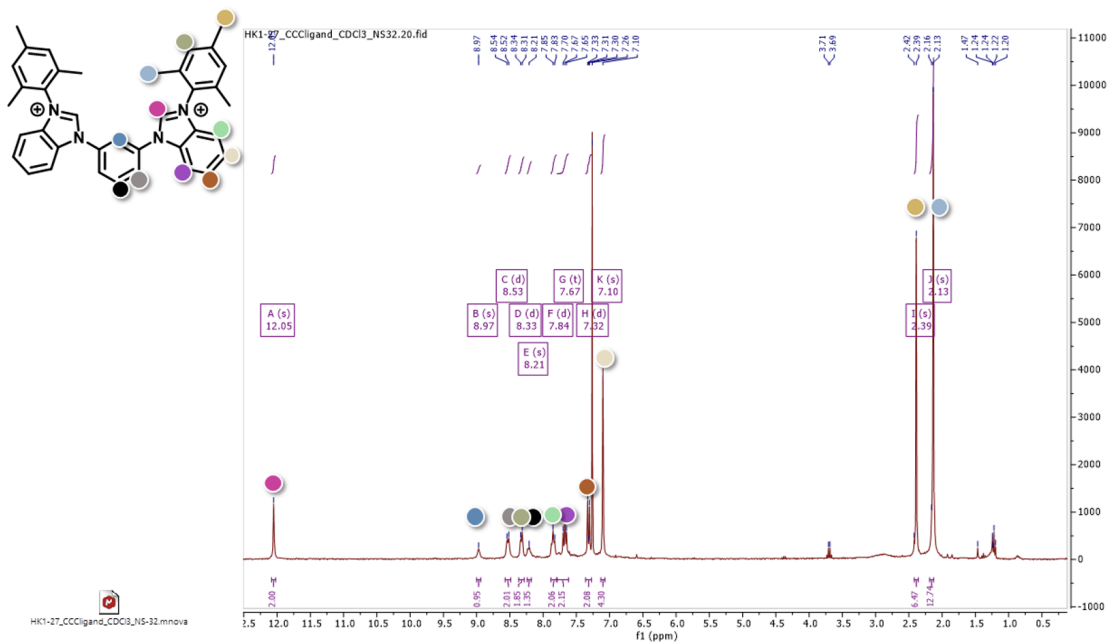
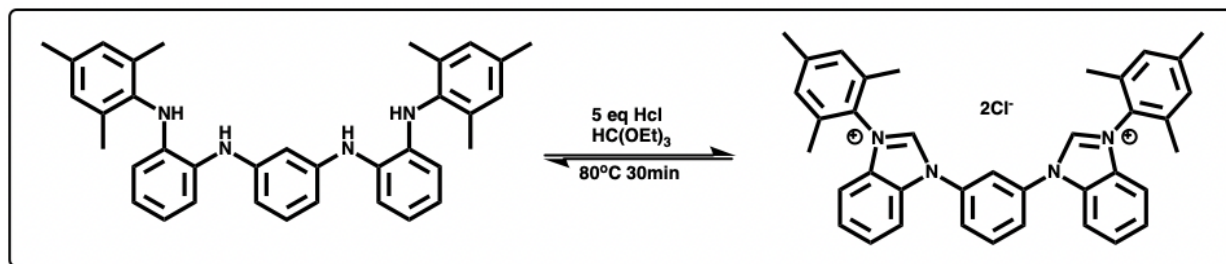


Figure 13: The NMR of Compound **(3)** with peak assignments.

The NMR of Compound **(3)** showed the correct product and came out mostly clean, with a few small impurities present. It had similar peaks to the previous two around 2.0-2.5 ppm for the methyl groups and 7.0-9.0 ppm for the cyclic groups. In addition, a peak was at 12.0 ppm due to the two nitrogens, one being a cation. So, we proceeded with the synthesis of the iridium CCC-pincer complex, Compound **(4)**.

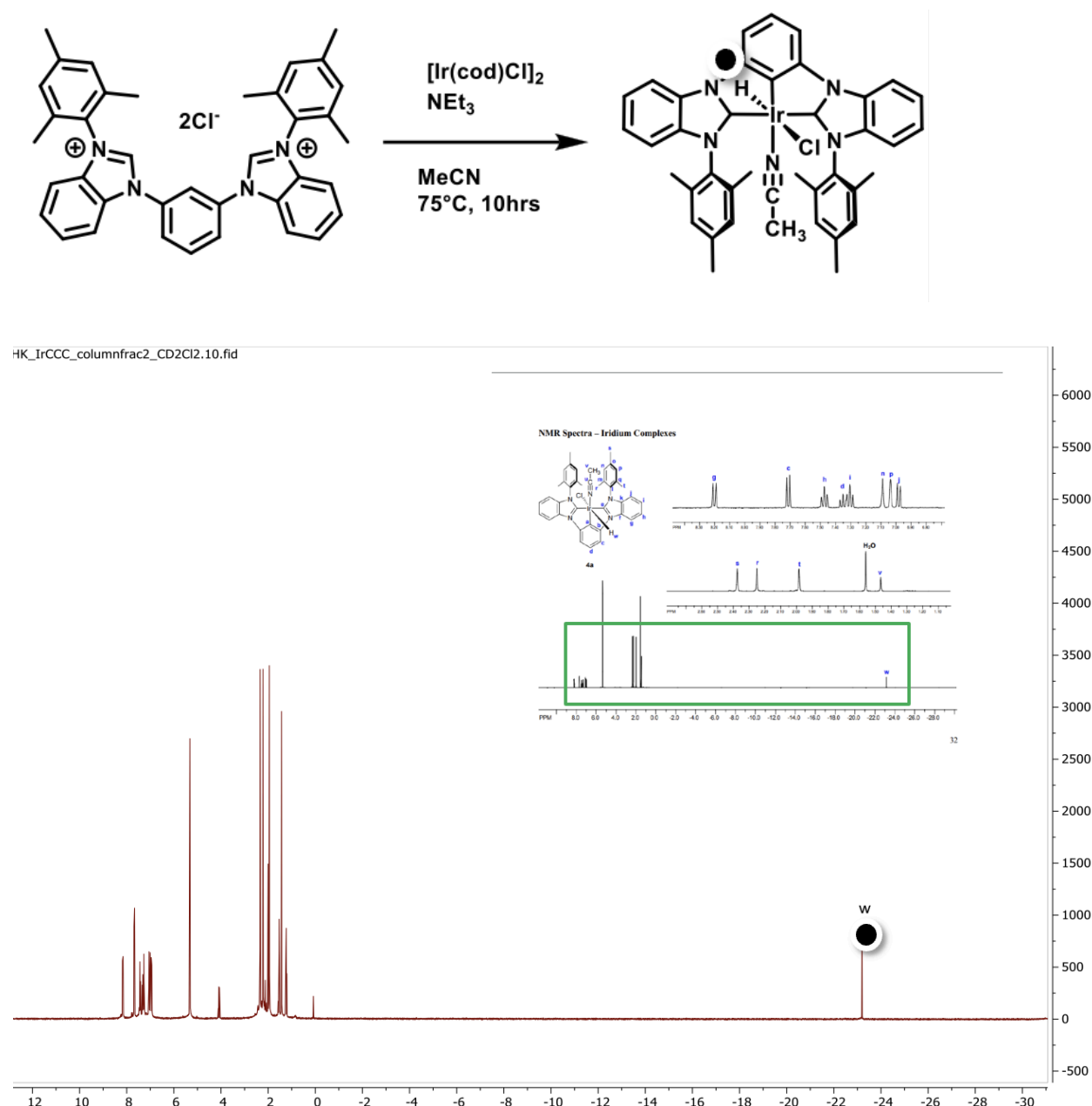


Figure 14: The NMR showing the hydride peak of the iridium CCC-pincer complex.

The peak for the hydride of the complex was largely negative, around -23 ppm. This was because the hydride was largely shielded by the bulky molecular structure of the pincer.

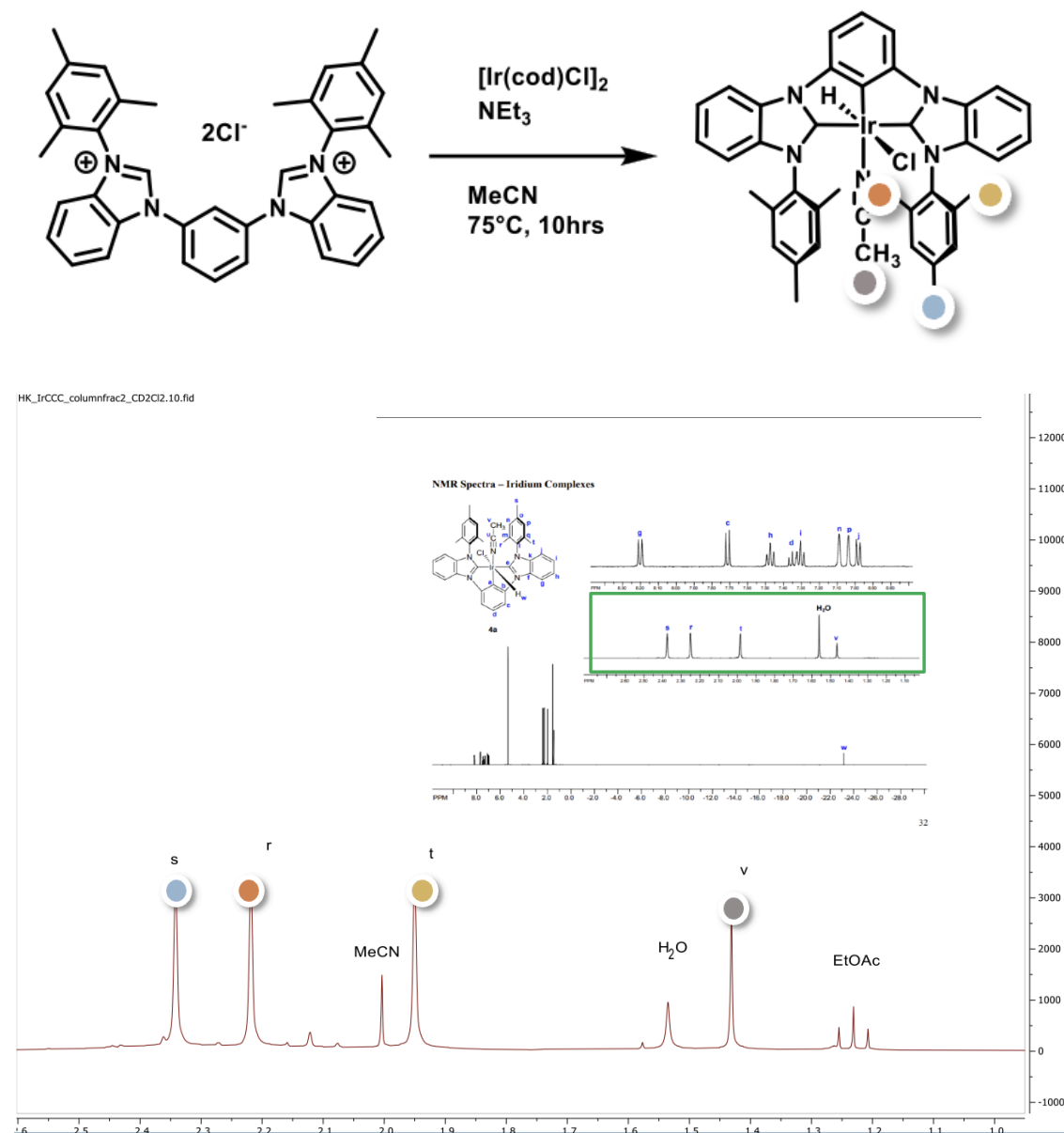
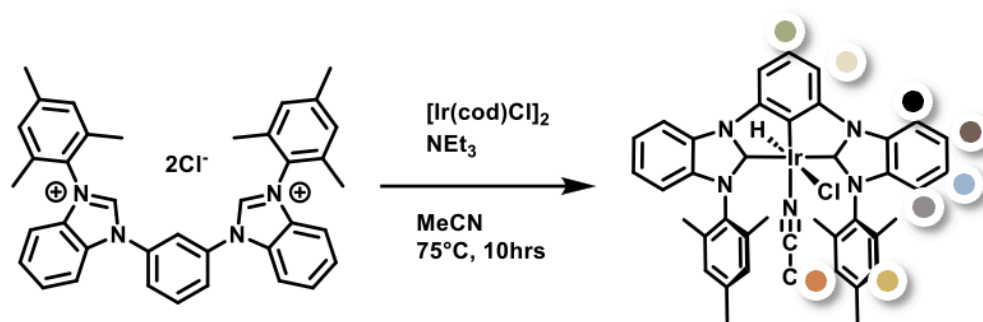
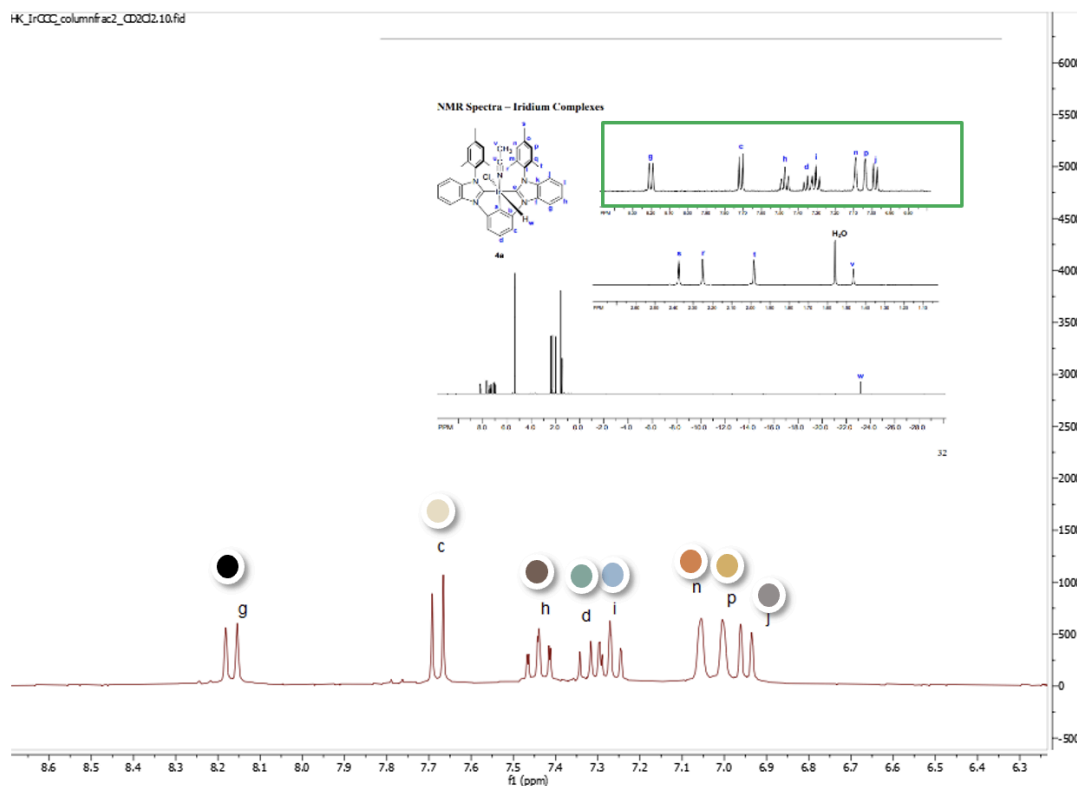


Figure 15: The NMR of the iridium CCC-pincer complex from the range of 1.0-2.5 ppm.

The peaks in this part of the NMR spectrum show the different methyl groups present on the compound, thus the lower ppm. In addition, it showed a handful of solvent impurities.



HK_IrCCC_columnfrac2_CD802.10.fid



Figures 16: The NMR of the iridium CCC-pincer complex from the range of 6.8-8.3 ppm.

The peaks in this part of the NMR spectrum showed the different benzyl groups of the pincer. The higher shifts were a result of the closer proximity to the nitrogen in the molecule.

The NMR of Compound (4) had a clear and prominent hydride peak integrating to 1H, indicating that we had the correct product. This meant that we were able to begin experimenting

on the redox properties of the iridium CCC-pincer complex and if it could perform the dehydrogenation reaction using a reducing agent.

Quantification of Octane Dehydrogenation

Using the resulting product of the in situ octane dehydrogenation, the internal standard of mesitylene was added, as well as the cyclohexane solvent, and was run through the GC-FID to determine if 1-octene was produced and to quantify the presence of octane and 1-octene in each mixture.

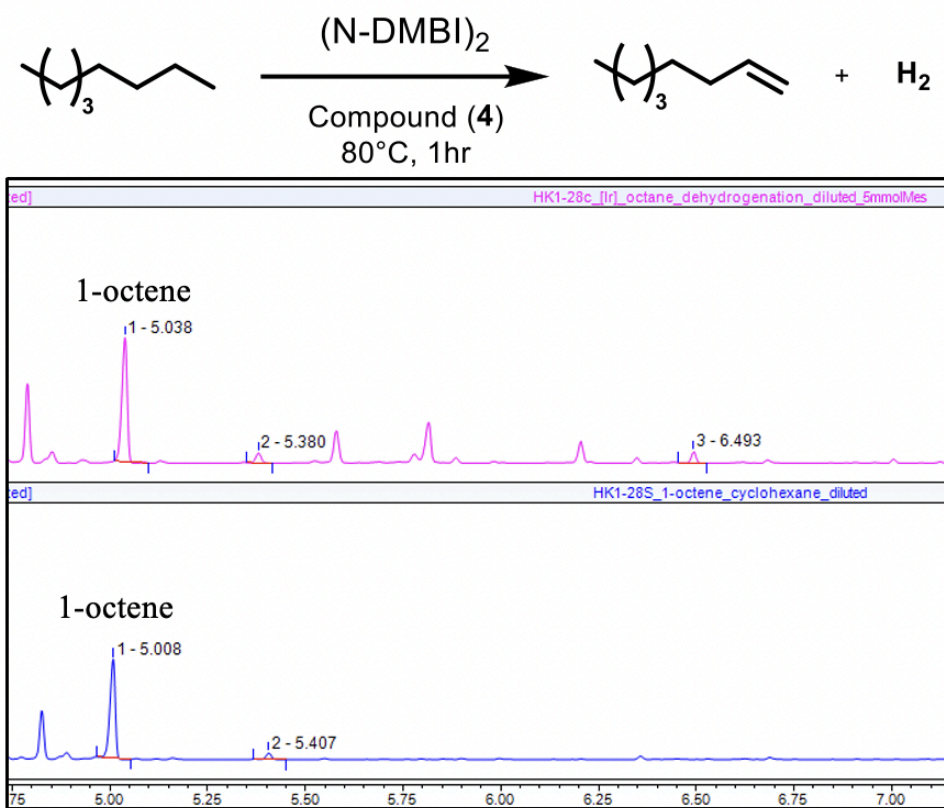


Figure 17: The GC-FID spectra for the solution with N-DMBI (pink) and without N-DMBI (blue).

The resulting spectra from the GC-FID seemed to contain many impurities and messy peaks. However, it was still identified that 1-octene was present in both solutions, with the solution containing N-DMBI having a greater quantity. While it was hypothesized that the solution without N-DMBI wouldn't produce 1-octene at all, it was most likely produced as a result of the strong base, triethylamine, being added at the same time, aiding in the oxidative addition step of the dehydrogenation mechanism.

I am currently making further efforts to redo the same reaction using the cleaner complex as well as cleaning the octane and cyclohexane used in the GC-FID. The expected result is to see 1-octene in the solution with N-DMBI and none in the solution without N-DMBI.

Conclusion

The aim of this study was to provide proof of concept of the ability of the iridium CCC-pincer complex to be reduced to perform the redox dehydrogenation catalytic reaction as a means to produce and store hydrogen. By proving the redox reaction can be done at ambient temperatures, the same reaction can be done using electrochemistry. My research has proven that more 1-octene was present in the reaction containing a reducing agent, N-DMBI, rather than the reaction without. This indicated that N-DMBI was able to successfully reduce the iridium metal center to perform the dehydrogenation reaction. However, the GC-FID spectra of these reactions were messy and the solvents used were dirty. So, future research will include cleaning the solvents and re-running the reaction in a more controlled environment to get cleaner results. In addition, if the proof of concept reaction provides the results we desire, we will move towards using electrochemistry to perform the same reaction. This project was in partnership with Nathan Neale at the National Renewable Energy Laboratories and future research will involve his team performing our electrochemical reaction using photochemistry.

References

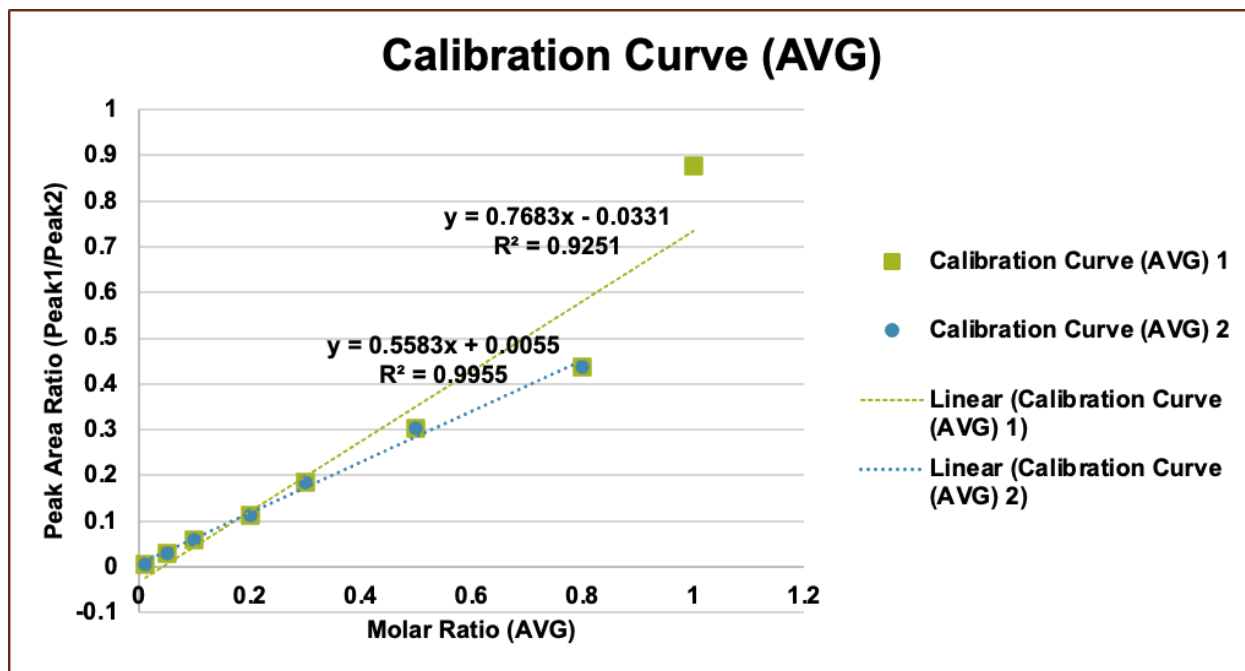
- (1) *AR4 Climate Change 2007: The Physical Science Basis — IPCC.*
<https://www.ipcc.ch/report/ar4/wg1/> (accessed 2024-03-09).
- (2) Lindsey, R. Climate Change: Atmospheric Carbon Dioxide | NOAA Climate.Gov. **2023**.
- (3) *Hydrogen Production: Natural Gas Reforming.* Energy.gov.
<https://www.energy.gov/eere/fuelcells/hydrogen-production-natural-gas-reforming>
(accessed 2023-08-23).
- (4) *Use of hydrogen - U.S. Energy Information Administration (EIA).*
<https://www.eia.gov/energyexplained/hydrogen/use-of-hydrogen.php> (accessed
2023-04-24).
- (5) *Safe Use of Hydrogen.* Energy.gov.
<https://www.energy.gov/eere/fuelcells/safe-use-hydrogen> (accessed 2024-03-09).
- (6) Sisáková, K.; Podrojková, N.; Oriňaková, R.; Oriňak, A. Novel Catalysts for
Dibenzyltoluene as a Potential Liquid Organic Hydrogen Carrier Use—A Mini-Review.
Energy Fuels **2021**, *35* (9), 7608–7623. <https://doi.org/10.1021/acs.energyfuels.1c00692>.
- (7) Gianotti, E.; Taillades-Jacquín, M.; Rozière, J.; Jones, D. J. High-Purity Hydrogen
Generation via Dehydrogenation of Organic Carriers: A Review on the Catalytic Process.
ACS Catal. **2018**, *8* (5), 4660–4680. <https://doi.org/10.1021/acscatal.7b04278>.
- (8) Chianese, A. R.; Drance, M. J.; Jensen, K. H.; McCollom, S. P.; Yusufova, N.; Shaner, S.
E.; Shopov, D. Y.; Tandler, J. A. Acceptorless Alkane Dehydrogenation Catalyzed by
Iridium CCC-Pincer Complexes. *Organometallics* **2014**, *33* (2), 457–464.
<https://doi.org/10.1021/om4006577>.
- (9) Uno, N.; Nakano, R.; Yamashita, M. Low-Temperature Dehydrogenation of Cyclooctane by

- Using Pincer Iridium Complexes Bearing an N,N'-Diarylated PNCNP Ligand. *ACS Catal.* **2023**, *13* (10), 6956–6965. <https://doi.org/10.1021/acscatal.3c01739>.
- (10) McKay, A. I.; Bukvic, A. J.; Tegner, B. E.; Burnage, A. L.; Martínez-Martínez, A. J.; Rees, N. H.; Macgregor, S. A.; Weller, A. S. Room Temperature Acceptorless Alkane Dehydrogenation from Molecular σ -Alkane Complexes. *J. Am. Chem. Soc.* **2019**, *141* (29), 11700–11712. <https://doi.org/10.1021/jacs.9b05577>.
- (11) Gao, Y.; Guan, C.; Zhou, M.; Kumar, A.; Emge, T. J.; Wright, A. M.; Goldberg, K. I.; Krogh-Jespersen, K.; Goldman, A. S. β -Hydride Elimination and C–H Activation by an Iridium Acetate Complex, Catalyzed by Lewis Acids. Alkane Dehydrogenation Cocatalyzed by Lewis Acids and [2,6-Bis(4,4-Dimethyloxazoliny)-3,5-Dimethylphenyl]Iridium. *J. Am. Chem. Soc.* **2017**, *139* (18), 6338–6350. <https://doi.org/10.1021/jacs.6b12995>.
- (12) Pham, P. H.; Barlow, S.; Marder, S. R.; Luca, O. R. Electricity-Driven Recycling of Ester Plastics Using One-Electron Electro-Organocatalysis. *Chem Catal.* **2023**, *3* (8), 100675. <https://doi.org/10.1016/j.checat.2023.100675>.
- (13) Tang, K.; Brown, M. R.; Risko, C.; Gish, M. K.; Rumbles, G.; Pham, P. H.; Luca, O. R.; Barlow, S.; Marder, S. R. Beyond N-Dopants for Organic Semiconductors: Use of Bibenzo[d]Imidazoles in UV-Promoted Dehalogenation Reactions of Organic Halides. *Beilstein J. Org. Chem.* **2023**, *19* (1), 1912–1922. <https://doi.org/10.3762/bjoc.19.142>.
- (14) Chianese, A. R.; Mo, A.; Lampland, N. L.; Swartz, R. L.; Bremer, P. T. Iridium Complexes of CCC-Pincer N-Heterocyclic Carbene Ligands: Synthesis and Catalytic C–H Functionalization. *Organometallics* **2010**, *29* (13), 3019–3026. <https://doi.org/10.1021/om100302g>.

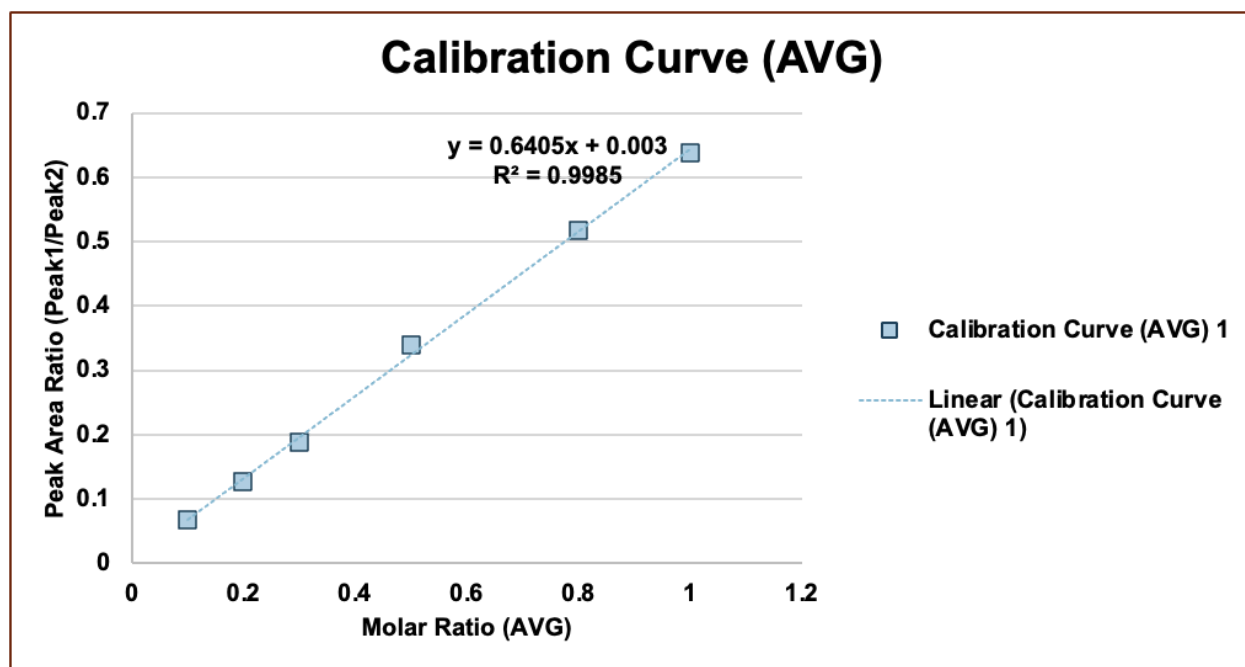
Appendix

Figures A1-A4) The calibration curves used to quantify the alkane/alkene quantities.

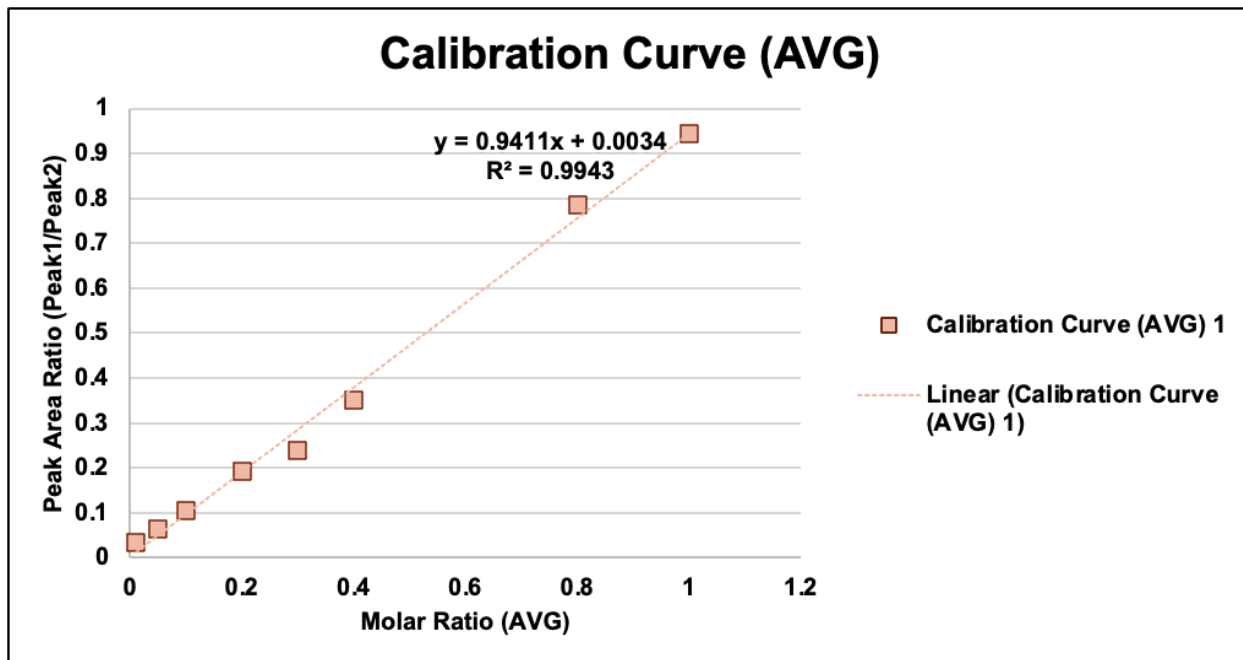
A1) Octane



A2) 1-Octene



A3) Cyclooctane



A4) cis-Cyclooctene

